



Figure 1. A Synthetic Image of the Microrectenna described in the text is here superimposed, to scale, on a real scanning electron micrograph of an insectlike microrobot. The underlying idea is to use the microrectenna to convert power from an incident 2.5-GHz radio beam to drive the robot and/or to charge its microbattery.

GaAs wafer. The resonant cavity renders the slot radiation pattern unidirectional with a half-power beam width of about  $65^\circ$ . A unique metal mesh on the rear of the wafer forms the backplate for the cavity but allows the GaAs to be wet etched from the rear surface of the twin slot antennas and ground plane. The beam leads protrude past the edge of the chip and are used both to mount the microrectenna and to make the DC electrical connection with external circuitry. The antenna ground plane and the components on top of it are formed on a  $2\text{-}\mu\text{m}$  thick GaAs membrane that is grown in the initial wafer MBE (molecular beam epitaxy) process. The side walls of the antenna cavity are not metal coated and, hence, would cause some loss of power; however, the relatively high permittivity ( $\epsilon=13$ ) of the GaAs keeps the cavity modes well confined, without the usual surface-wave losses associated with thick dielectric substrates.

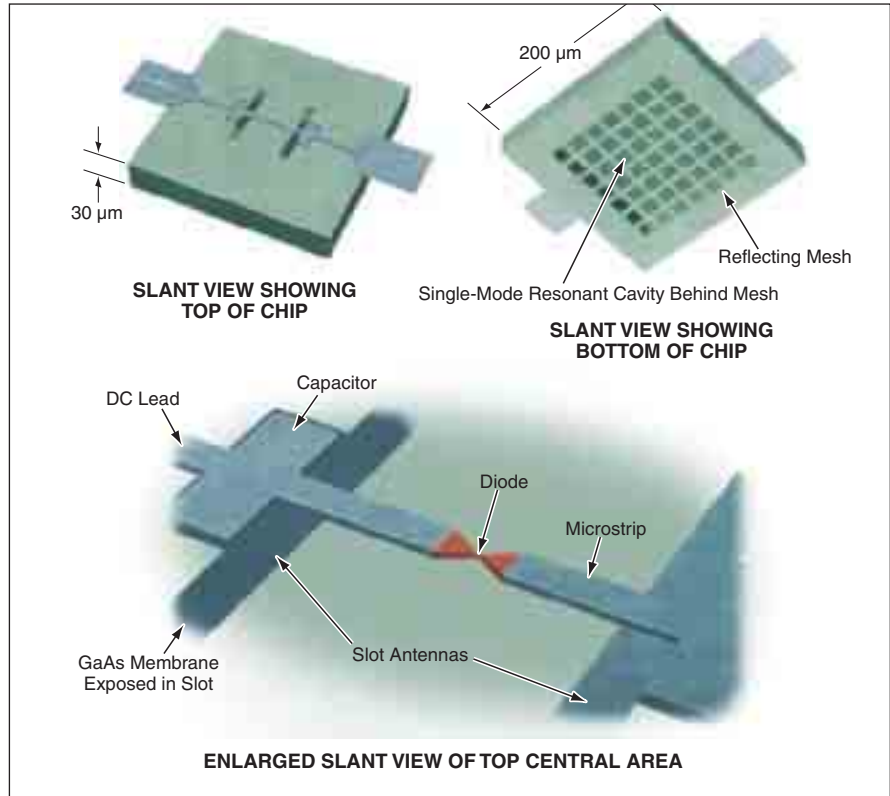


Figure 2. All RF and DC Components of the microrectenna would be fabricated together on a single GaAs chip.

The Schottky-barrier diode has the usual submicron dimensions associated with THz operation and is formed in a mesa process above the antenna ground plane. The diode is connected at the midpoint of a microstrip transmission line, which is formed on  $1\text{-}\mu\text{m}$ -thick SiO (permittivity of 5) laid down on top of the GaAs membrane. The twin slots are fed in phase by this structure. To prevent radio-frequency (RF) leakage past the slot antennas, low-loss capacitors are integrated into the microstrip transmission line at the edges of the slots. The DC current-carrying lines extend from the outer

edges of the capacitors, widen approaching the edges of the chip, and continue past the edges of the chip to become the beam leads used in tacking down the devices. The structure provides a self-contained RF to DC converter that works in the THz range.

*This work was done by Peter Siegel of Caltech for NASA's Jet Propulsion Laboratory.*

*This invention is owned by NASA, and a patent application has been filed. Inquiries concerning nonexclusive or exclusive license for its commercial development should be addressed to the Patent Counsel, NASA Management Office-JPL. Refer to NPO-30478.*

## Miniature L-Band Radar Transceiver

Numerous interdependent considerations are reflected in a compact, low-power, radiation-hard design.

NASA's Jet Propulsion Laboratory, Pasadena, California

A miniature L-band transceiver that operates at a carrier frequency of 1.25 GHz has been developed as part of a generic radar electronics module (REM) that would constitute one unit in an array of many identical units in a very-large-aperture phased-array antenna. NASA and the Department of Defense are considering the deploy-

ment of such antennas in outer space; the underlying principles of operation, and some of those of design, also are applicable on Earth. The large dimensions of the antennas make it advantageous to distribute radio-frequency electronic circuitry into elements of the arrays. The design of the REM is intended to implement the distribution.

The design also reflects a requirement to minimize the size and weight of the circuitry in order to minimize the weight of any such antenna. Other requirements include making the transceiver robust and radiation-hard and minimizing power demand.

Figure 1 depicts the functional blocks of the REM, including the L-band trans-

ceiver. The key functions of the REM include signal generation, frequency translation, amplification, detection, handling of data, and radar control and timing. An arbitrary-waveform generator that includes logic circuitry and a digital-to-analog converter (DAC) generates a linear-frequency-modulation chirp waveform. A frequency synthesizer produces local-oscillator signals used for frequency conversion and clock signals for the arbitrary-waveform generator, for a digitizer [that is, an analog-to-digital converter (ADC)], and for a control and timing unit. Digital functions include command, timing, telemetry, filtering, and high-rate framing and serialization of data for a high-speed scientific-data interface.

The aforementioned digital implementation of filtering is a key feature of the REM architecture. Digital filters, in contradistinction to analog ones, provide consistent and temperature-independent performance, which is particularly important when REMs are distributed throughout a large array. Digital filtering also enables selection among multiple filter parameters as required for different radar operating modes. After digital filtering, data are decimated appropriately in order to minimize the data rate out of an antenna panel.

The L-band transceiver (see Figure 2) includes a radio-frequency (RF)-to-baseband down-converter chain and an intermediate-frequency (IF)-to-RF up-con-

verter chain. Transmit/receive (T/R) switches enable the use of a single feed to the antenna for both transmission and reception. The T/R switches also afford a built-in test capability by enabling injection of a calibration signal into the receiver chain. In order of decreasing priority, components of the transceiver were selected according to requirements of radiation hardness, then compactness, then low power. All of the RF components are radiation-hard. The noise figure (NF) was optimized to the extent that (1) a low-noise amplifier (LNA) (characterized by  $NF < 2$  dB) was selected but (2) the receiver front-end T/R switches were selected for a high degree of isolation and acceptably low loss, regardless of the requirement to minimize noise.

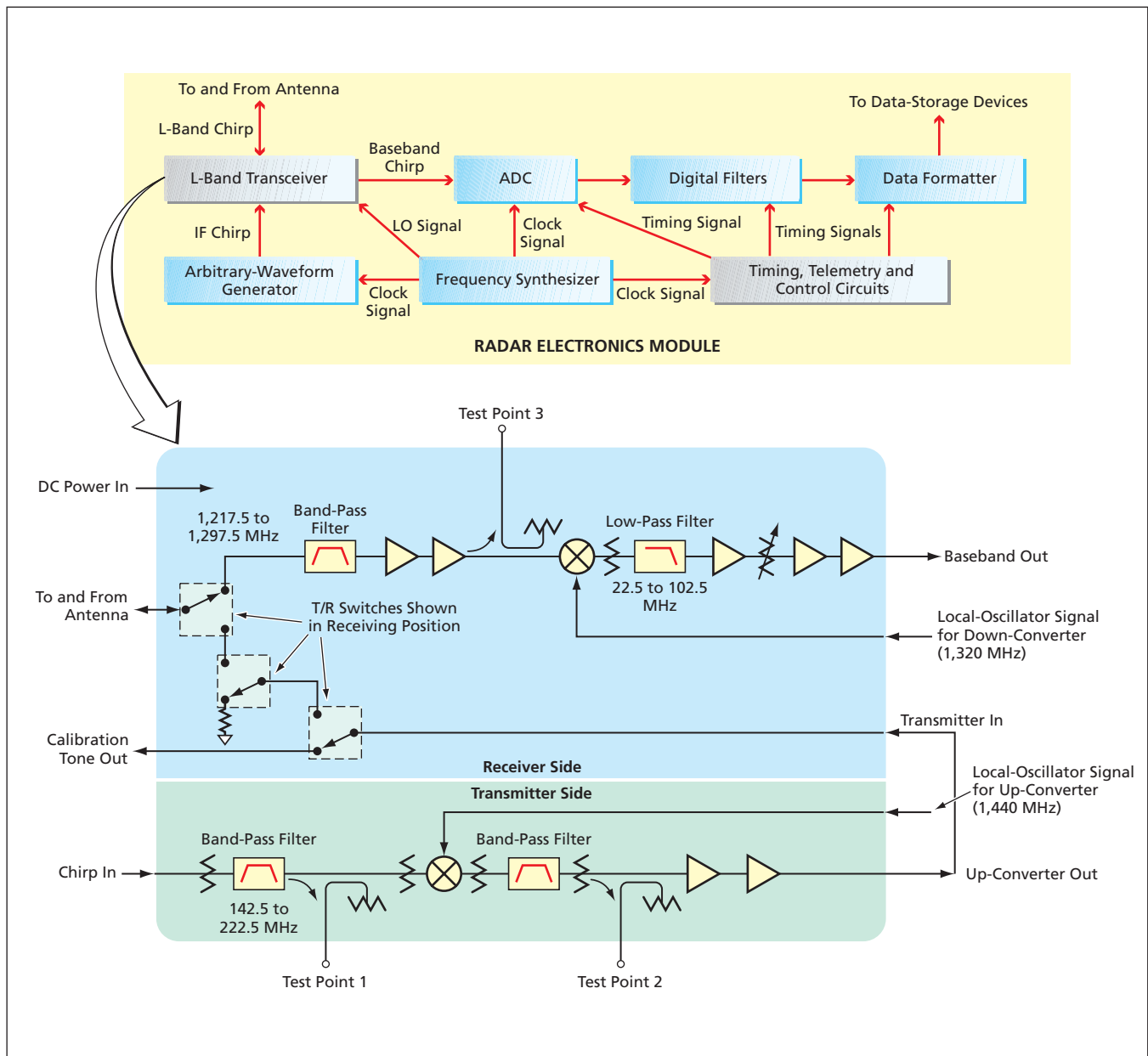


Figure 1. The Radar Electronics Module contains the miniature L-band transceiver.

The filter specifications were chosen to minimize the sizes of the filters, thereby placing the baseband higher in frequency than would otherwise be necessary. This is an acceptable trade-off inasmuch as (1) the consequent requisite digitizer bandwidth is still realizable by use of commercial devices and (2) the decimation performed by the digital filters eliminates excess bandwidth. The receiver band-pass filter (BPF) is placed in front of the LNA in order to limit radio-frequency interference. A programmable attenuator is included to provide adequate dynamic range in the event that the amplitude of the radar echo varies significantly. Care was taken to minimize cost by minimizing the number of parts and the number of different types of parts: in particular, the amplifiers and mixer used in the up-converter are also used in the down-converter.

The packaging of the L-band transceiver was designed in recognition that the different types of electronic devices used must be mounted and connected in different ways. The packaging approach was to place circuits that perform different functions in separate cavities in the module housing, coupling the DC signals through the walls by use of filtered connections only. This ap-

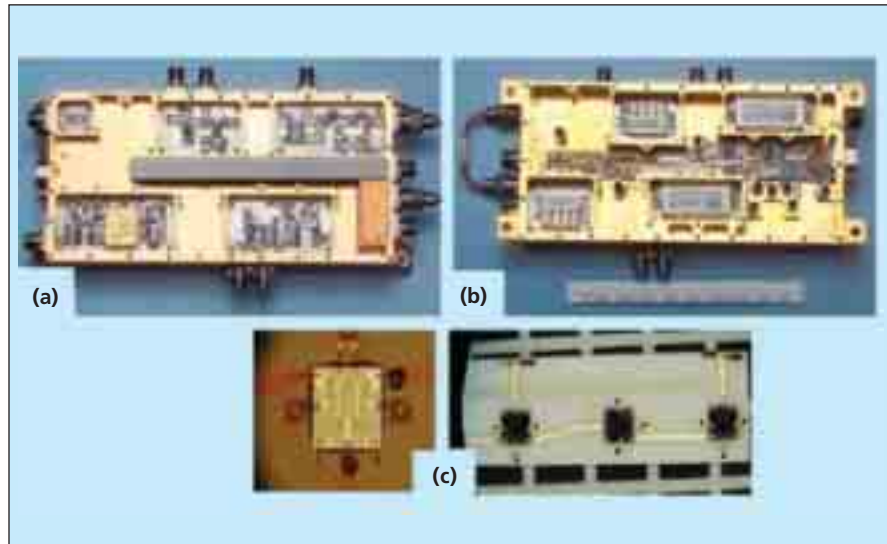


Figure 2. The Uncovered L-Band Transceiver Module shows the following: (a) top view (active components), (b) bottom view (filters and control), and (c) close-up views of packaging of individual switch die circuitry.

proach provides shielding from noise leakage. Thus, the down-converter (receiver) chain, the up-converter (transmitting) chain, and the control and power-supply circuitry are each located in separate cavities of the housing. The active RF components (e.g., amplifiers) are on one side of the module, while the passive RF components (e.g., attenuators and filters) and the control and

power circuits are on the opposite side. The RF functional blocks are further separated, according to frequency, onto individual substrates and into individual cavities.

*This work was done by Dalia McWatters, Douglas Price, and Wendy Edelstein of Caltech for NASA's Jet Propulsion Laboratory. For more information, contact iaoffice@jpl.nasa.gov. NPO-41278*

## Robotic Vision-Based Localization in an Urban Environment

A probability distribution of location is superimposed on an approximate map.

NASA's Jet Propulsion Laboratory, Pasadena, California

A system of electronic hardware and software, now undergoing development, automatically estimates the location of a robotic land vehicle in an urban environment using a somewhat imprecise map, which has been generated in advance from aerial imagery. This system does not utilize the Global Positioning System and does not include any odometry, inertial measurement units, or any other sensors except a stereoscopic pair of black-and-white digital video cameras mounted on the vehicle. Of course, the system also includes a computer running software that processes the video image data.

The software consists mostly of three components corresponding to the three major image-data-processing functions:

- *Visual Odometry*

This component automatically tracks point features in the imagery and computes the relative motion of the cam-

eras between sequential image frames. This component incorporates a modified version of a visual-odometry algorithm originally published in 1989. The algorithm selects point features, performs multiresolution area-correlation computations to match the features in stereoscopic images, tracks the features through the sequence of images, and uses the tracking results to estimate the six-degree-of-freedom motion of the camera between consecutive stereoscopic pairs of images (see figure).

- *Urban Feature Detection and Ranging*

Using the same data as those processed by the visual-odometry component, this component strives to determine the three-dimensional (3D) coordinates of vertical and horizontal lines that are likely to be parts of, or close to, the exterior surfaces of buildings. The basic sequence of processes performed by this component is the

following:

1. An edge-detection algorithm is applied, yielding a set of linked lists of edge pixels, a horizontal-gradient image, and a vertical-gradient image.
2. Straight-line segments of edges are extracted from the linked lists generated in step 1. Any straight-line segments longer than an arbitrary threshold (e.g., 30 pixels) are assumed to belong to buildings or other artificial objects.
3. A gradient-filter algorithm is used to test straight-line segments longer than the threshold to determine whether they represent edges of natural or artificial objects. In somewhat oversimplified terms, the test is based on the assumption that the gradient of image intensity varies little along a segment that represents the edge of an artificial object.